The Meteorological Magazine

September 1990

The Great Storm: passive microwave evaluations
Heavy mesoscale snowfall in northern Germany

Met.O.992 Vol. 119 No. 1418

The Meteorological Magazine

September 1990
Vol. 119 No. 1418

551.501.795:551.515.12:551.553.8(261.2+261.26+41): 551.577.37:551.465.75

The Great Storm of 15/16 October 1987: passive microwave evaluations of associated rainfall and marine wind speeds

E.C. Barrett, C. Kidd, and J.O. Bailey
Remote Sensing Unit, Department of Geography, University of Bristol
C.G. Collier
Meteorological Office, Bracknell

Summary

The Special Sensor Microwave Imager (SSM/I) carried by current US military meteorological satellites has proven capabilities for the evaluation of several weather and weather-related parameters, including instantaneous rain areas and rain rates, and marine wind speeds. Analyses of SSM/I data for the British Isles and surrounding waters from 15–16 October 1987 throw new light upon the Great Storm at its peak intensity, and raise the possibility of improved forecasting of such events in the future.

1. Introduction

Much has already been written on the Great Storm which struck southern Britain on the night of 15/16 October 1987 (see Fig. 1 for synoptic charts). At least 18 people lost their lives as a direct result of the gale, hundreds of millions of pounds worth of damage resulted, and millions of trees were blown down in what the Home Secretary described as '...the worst, most widespread night of disaster in the south-east of England since 1945'. In one sense the extreme events of January/February 1990 have since at least partially diverted attention from the Great Storm of 1987, but in another sense these subsequent events have only heightened interest in, and concern for, severe events of this nature. It is therefore even more important than before that such events should be studied in as much detail as possible, and using all the facilities at our disposal. Clearly meteorological satellites have an important part to play in helping to evaluate and forecast potentially dangerous weather systems approaching the British Isles from the North Atlantic. The use of NOAA, and more particularly Meteosat, satellite data in these respects is by now well established and widely appreciated. Fortunately, the technology of meteorological satellites is not standing still, and recent advances in satellite instrumentation are opening up new possibilities of monitoring features of North Atlantic depressions which were previously not amenable, or easily amenable, to elucidation using satellite data. This paper seeks to present some new information concerning the Great Storm of 15/16 October 1987, as seen by the newest member of the US Military Defense Meteorological Satellite Program (DMSP) satellite family, through the eyes of its Special Sensor Microwave Imager (SSM/I), the newest and most promising passive microwave imaging radiometer (see Barrett *et al.* 1988).

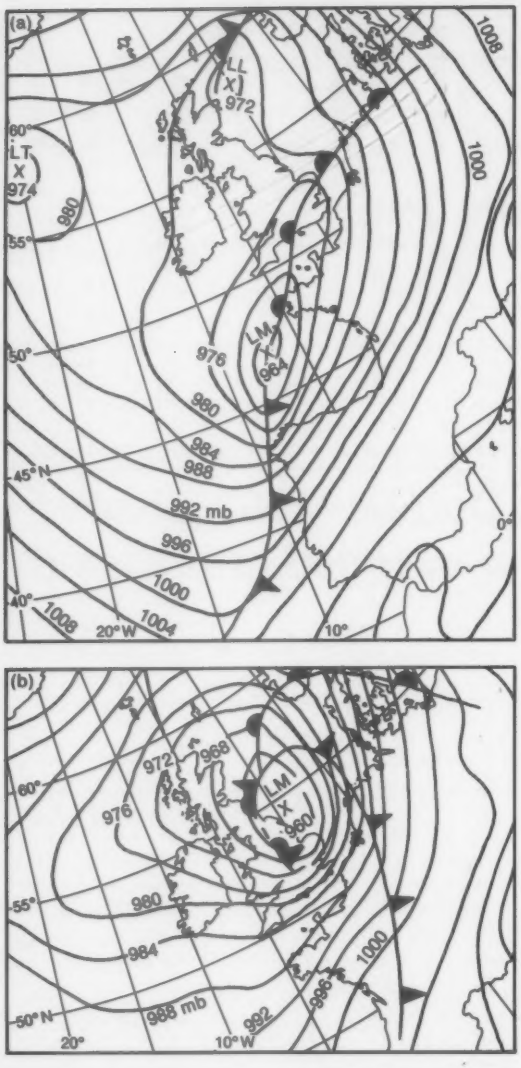

Figure 1. Synoptic weather maps for (a) 1800 UTC on 15 October 1987, and (b) 0600 UTC on 16 October 1987.

2. Satellite passive microwave radiometers

Table I gives details of those satellite microwave imaging instruments which have flown on meteorological satellites since the early 1970s, and have provided data to which the general scientific community has had at least some access. Of these, the first three (ESMR-5, ESMR-6 and SMMR) all flew on Nimbus satellites, and all are now defunct. However the fourth (the SSM/I), part of the payload of the current DMSP Block 5D-2 spacecraft F8, is both currently functional, and a significant advance over previous passive microwave imaging instruments. Launched on 19 June 1987, this DMSP satellite occupies a circular, sun-synchronous near-polar orbit at an altitude of 833 km, with an inclination of 98.8° to the equator, and an orbital period of 102.0 min. The satellite has an ascending node equatorial crossing time of 06.12 hrs, and provides an observation swath width of 1394 km. The SSM/I instrument, as detailed in Table I, is a standardized channel, 4-frequency, linearly polarized, passive microwave radiometric system (Hollinger *et al.* 1987). Built by the Hughes Aircraft Company under the direction of the US Naval Space Systems Activity and the US Air Force Space Division, the SSM/I was designed primarily to support operational environmental products prepared by the US Fleet Numerical Oceanography Command and the US Air Force Weather Center. Fortunately, despite the military origin of SSM/I, its data are being archived by the Satellite Data Services Division of NOAA/NESDIS (National Environmental Satellite and Data Information System), from whence they will soon be available to the general scientific community for research and algorithm development. In the meantime, quantities of SSM/I data have been made available to the Remote Sensing Unit in the University of Bristol (RSUUB) under a co-operative agreement between them and NOAA/NESDIS (Satellite Applications Laboratory), and under the auspices of the NASA-led WetNet project, in which the RSUUB is involved.

The SSM/I represents an advance over previous instruments in that it is the first sensor equipped to monitor in the 85.5 GHz region, it has a much broader swath width than previous instruments, it is in continuous operation, its data have been more directly calibrated, its feed horn antenna are in synchronous rotation (eliminating the need for polarization rotation corrections), its noise levels are lower, and the footprints from all its channels enjoy co-aligned sampling.

It will be seen from Table I that the SSM/I is intended for use in respect of a variety of meteorological and geophysical parameters, including ocean wind speed and intensity of precipitation. Whilst the earliest studies based upon the SSM/I in the RSUUB have focused primarily upon rainfall (e.g. Kidd *et al.* 1989), this paper seeks to explore the value of the instrument for both wind speed and rainfall estimation in the vicinity of the British Isles for extreme weather conditions using the Great Storm of October 1987 as an interesting test case. Fig. 2 presents false-colour images of the Great Storm using yellow, green and blue to represent vertical polarization data (V), horizontal polarization data (H), and the vertical minus horizontal polarization difference, respectively, all at 85.5 GHz.

3. Application of an SSM/I wind-speed algorithm

Extraction of the wind-speed parameter from passive microwave radiometer data was discussed in Munn (1978) and Swift (1977) where it is demonstrated that wind speeds near the ocean surface can be remotely sensed by both scatterometers and microwave radiometers, in the first case by measuring the component of transmitted power that is back-scattered from the ocean

Table I. Satellite passive microwave imaging instruments (from Bailey *et al.* 1986)

Instrument	ESMR-5	ESMR-6	SMMR	SSM/I
Spacecraft launch date	Nimbus-5 December 1972	Nimbus-6 June 1975	Nimbus-7/Seasat October/June 1978	DMSP 5D-2/SX June 1987
Frequencies/ footprint sizes				
6.6 GHz	—	—	VH 121 × 79 km	—
10.7 GHz	—	—	VH 74 × 49 km	—
18.0 GHz	—	—	VH 44 × 29 km	—
19.35 GHz	X 25 × 25 km	—	—	VH 69 × 43 km
21.0 GHz	—	—	VH 38 × 25 km	—
22.235 GHz	—	—	—	V 50 × 40 km
37.0 GHz	—	VH 25 × 45 km	VH 21 × 14 km	VH 37 × 28 km
85.5 GHz	—	—	—	VH 15 × 13 km
Primary aims of mission	Liquid water contents of clouds, sea ice and open sea coverage. Surface composition and soil type, with surface features and surface moisture.		Sea surface temperature, near sea surface winds. Water vapour, liquid water content and cloud droplet size. Rainfall rate.	Ocean wind speed and ice coverage, age, and extent. Intensity of precipitation, cloud water content and land surface moisture.

Key: ESMR = Electrically Scanning Microwave Radiometer, SMMR = Scanning Multi-channel Microwave Radiometer, SSM/I = Microwave Imager, V = vertical polarization, H = Horizontal polarization, and X = non-polarized.

surface, and in the second by measuring radiation naturally emitted from the ocean surface. Both the backscattered radiation and emitted radiation are affected directly by ocean surface roughness, which is, in turn, related to the near-surface wind speed.

Detailed empirical work has been reported by Wentz *et al.* (1986) in which wind speed results were obtained from a Seasat scatterometer algorithm and compared with wind speed measurements from US National Data Buoy Office buoy observations. A total of 1623 buoy wind speed/Seasat results were compared, and the agreement was such that an r.m.s. discrepancy of only 1.6 m s^{-1} was found. The correlation coefficient of 0.89 suggested a high level of association between the two variables despite such factors as temporal and spatial sampling problems. These results were then used to assess the performance of a brightness temperature (T_b) model based on Nimbus-7 Scanning Multi-channel Microwave Radiometer (SMMR) data. Wentz cites the results of 123 000 wind-speed comparisons between the two methods for T_b algorithms using different channel combinations, for which he found generally good agreements. For the most favourable channel combinations, this agreement was broadly within 1.3 m s^{-1}. Taking into account the improvements in design that were to be incorporated in the SSM/I microwave radiometer, Wentz confidently predicted that, using appropriate channel combinations, near-surface wind speeds should be determinable usually to within 2 m s^{-1} with the new instrument.

The SSM/I wind-speed extraction algorithm of Hollinger *et al.* (1987) (portrayed in Fig. 3), which includes different weights for different latitudes and seasons of the year, fulfils Wentz's expectations. Based on the 19H, 22V, 37V and 37H channel data (19H, 22V, etc. are channel reference numbers) with a spatial resolution of 25 km and a range of values from 3–25 m s^{-1}, the Hollinger algorithm yields wind-speed products with a claimed accuracy of ±2 m s^{-1}. Early analyses of SSM/I wind speed algorithm outputs by Wentz (personal communication) using this algorithm confirm that results obtained have indeed been to this general level of accuracy.

There are, however, reasons to believe that because of a number of physical conditions, properties and associated processes, care must be taken in the application of the SSM/I algorithm for wind speed. As early as 1971 Nordberg, using data from the SMMR on a Nimbus-7, indicated that even over open water the T_b value is affected by a number of factors, especially the ocean surface emissivity E, and that changes in E were non-linear with respect to wind speed because the T_b value measured by the satellite is affected by both the wind-induced surface roughness, and the presence of foam at the surface (Nordberg *et al.* 1971). Nordberg's results suggested that the T_b increased linearly with wind speeds above 7 m s^{-1}, mainly due to the presence of foam, whilst below 7 m s^{-1} no foam forms. The relationship of wind speed to T_b observed by Hollinger using SSM/I data is shown in Fig. 3. Since ship-borne

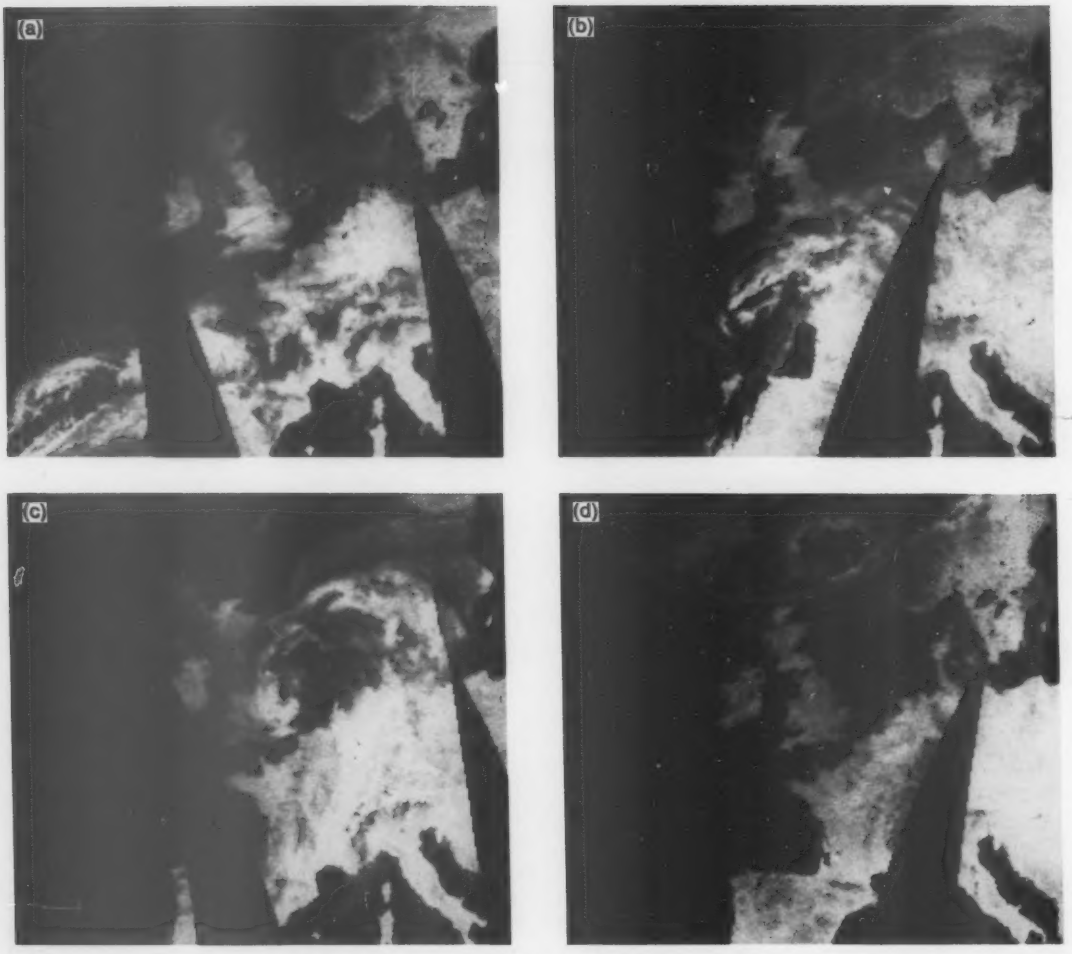

Figure 2. False-colour images of SSM/I swaths for (a) the evening of 15 October, (b) the morning of 16 October, (c) the evening of 16 October, and (d) the morning of 17 October, showing stages in the development and dissipation of the Great Storm as it moved north-east from the Bay of Biscay, across the British Isles, to the north-east of Scotland. Green areas are mainly hydrometeors and the most likely to be precipitating; cloud cover on all four occasions was much broader than the areas of hydrometeors.

wind measurements are standardized to a height of 20 m above the ocean surface, whereas the microwave observation is for the ocean-air interface, Hollinger *et al.* (1987) sought to extrapolate from the surface measurement of the SSM/I to a height of 20 m using a relationship developed by Cardone (1969).

Further complications are likely where radiometer cell values are contaminated by the presence of land or sea-ice; indeed, at present it seems prudent not to attempt wind-speed estimation in cells containing either of these features. Further, it has been suggested that when rain occurs wind speed estimates may be in error (Wentz 1988), although the degree to which the wind speed estimate is degraded by rain is still uncertain. In view of the physical principles underpinning the algorithm in question, it seems likely that useful wind-speed estimates should be obtainable, at least providing rain is light.

Notwithstanding the above problems, all of which call for detailed future examination, wind-speed products have been prepared using the image processing system in the RSUUB for the evening of 15 October 1987, and the morning of 16 October 1987. The mid-latitude spring/autumn relationships in the Hollinger algorithm have been used, the winds being contoured in knots to facilitate intercomparisons with numerical weather analyses, as presented and discussed below. The results are shown in Fig. 4. In Fig. 4(a) the highest values appear in the Bay of Biscay, reaching over 61 kn in places. High wind speeds are evident in some windward coastal regions, including the west coast of France, the Strait of Dover, and even parts of the west coast of Norway. The lowest wind speeds (below 20 kn) are found to the south-west of Ireland, corresponding with the location of the weak col in that position at that time. In Fig. 4(b), by which time the Great Storm vortex

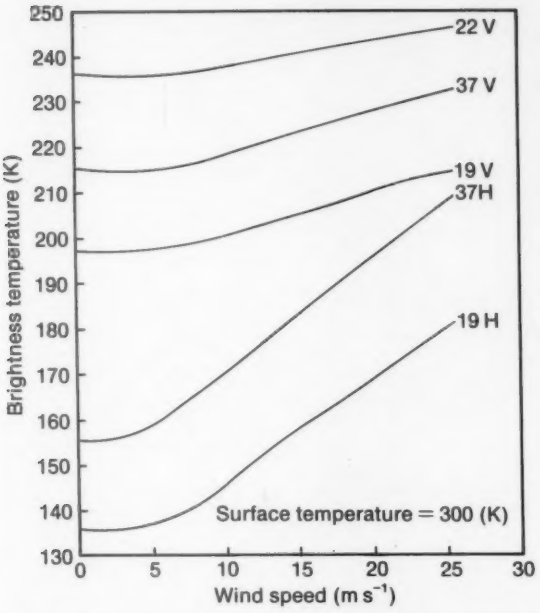

Figure 3. The relationship between wind speed and the SSM/I-derived brightness temperatures, for various channels, as found by Hollinger *et al.* (1987).

centre was over the north-eastern Midlands, wind speeds had increased along the North Sea coasts of England and Scotland, very locally seeming to exceed 61 kn in The Wash and off the Forth Estuary. The maps in Fig. 5 are constructed in the RSUUB from the Meteorological Office fine-mesh model wind analyses for 18 UTC on 15 October (Fig. 5(a)), and 06 UTC on 16 October (Fig. 5(b)) for times approximately one hour before the evening SSM/I overpass, and one hour after the morning SSM/I overpass respectively.

Allowing for the time differences between the model and satellite products, an intercomparison of Figs 4 and 5 reveals the following:

(a) The ranges of wind speeds from the analytical model and the satellite image analyses are similar, the model maxima being in excess of 50 kn compared with the satellite maxima in excess of 60 kn; the satellite minima are also generally higher (sometimes considerably higher) than the model minima especially near centres of positive vorticity.

(b) The model and satellite patterns of wind speeds for the evening of 15 October show many general similarities, including maxima in the Bay of Biscay, the southern North Sea, and in the region of Orkney and Shetland, and minima to the west of Ireland and the east of Scotland and north-east England. However, relative differences occur over some large areas, e.g. the southern North Sea versus the region of Orkney and Shetland (the model evaluating the

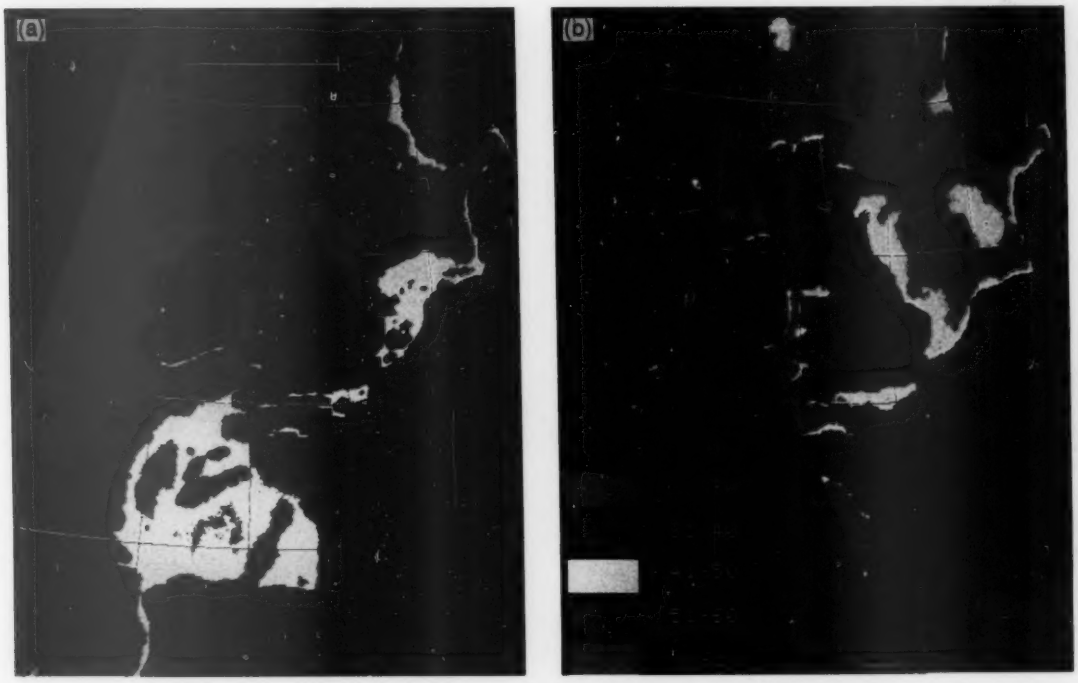

Figure 4. SSM/I-derived wind speeds (kn) for the seas surrounding the British Isles on (a) 15 October at approximately 1900 UTC, and (b) 16 October at approximately 0500 UTC, using the Hollinger *et al.* (1987) algorithm for mid-latitude in spring/autumn.

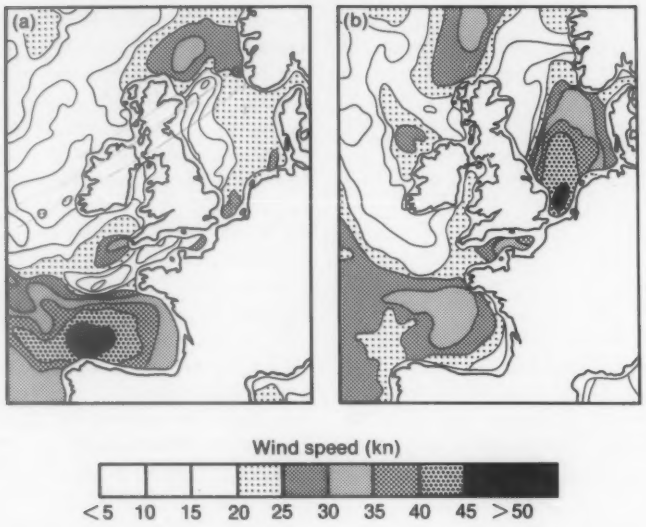

Figure 5. Wind speeds (kn) for (a) 18 UTC on 15 October, and (b) 06 UTC on 16 October 1987, compiled from the Meteorological Office fine-mesh model.

former as the windier of the two, whilst the satellite suggests the reverse relationship). Further, quite strong detail differences occur in a few areas, e.g. the Strait of Dover and the exposed coasts of western France, where the satellite estimates are more than double the model estimates.

(c) The model and satellite patterns of wind speeds for the morning of 16 October show more differences than (b), the satellite estimates again tending to be generally higher, although the model gives higher wind speeds in the southern North Sea. Otherwise the most notable difference perhaps is in the Forth Estuary region, where the model suggests light onshore winds and the satellite strong winds. It seems likely that the one-hour lag between the satellite image and the model outputs has been more obviously important in this case, for within that hour the area of maximum wind speed seems to have moved from the land into the southern North Sea.

4. Application of an SSM/I rainfall algorithm

It is now well known that, at certain frequencies, passive microwave radiation from the earth–atmosphere system relates to hydrometeors in the atmosphere, permitting estimation of instantaneous rain-rates (see Barrett and Martin 1981). Because the physical relationships between the radiation observed by the satellite and the precipitation process are more direct in the case of passive microwave than visible and/or infra-red radiation observed from satellite altitudes, it is expected that passive microwave sensors such as SSM/I will prove much better for rainfall monitoring than any visible and/or infra-red sensors, which are only able to observe radiation reflected or emitted from cloud tops. Early work based upon SMMR imagery was undertaken by Wilheit *et al.* (1977) who calculated radiative properties of hydrometeors in the atmosphere, and Savage (1978) who computed the radiative properties of hydrometeors at microwave frequencies from 20 to 183 GHz. As a result of these works, and others which have added further detail, it is now recognized that rain areas can be detected by passive microwave imagery within the region from about 6 to 90 GHz. This is the result of absorption and emission from raindrops below about 22 GHz, by the scattering from larger particles, raindrops and/or ice crystals above about 60 GHz, and by either or both processes between 22 and 60 GHz as determined by the actual occurrence, nature and quantity of both liquid droplets and ice particles (Bailey *et al.* 1986).

Investigations into rainfall monitoring using passive microwave image data were first concentrated over the oceans. Here the water surface provides a low background temperature which is essentially uniform, for the emissivity and absolute temperature of ocean surfaces are inversely proportional to each other. Over such areas, at low frequencies, the presence of precipitation causes an increase in the T_b because of emission from water droplets in the atmosphere, producing 'warm' islands seen against 'cold' ocean surfaces. Indeed, it has been found that, for a wide range of over-water rain-rates, there is an almost linear relationship between rain-rates and observed T_b values. Therefore, it has proved possible to develop simple algorithms for rainfall retrieval over oceans using data at frequencies less than 22 GHz. The most extensive work of this nature was undertaken by Rao (1984), who had produced a global atlas of oceanic precipitation (Rao *et al.* 1976) based on data from the Nimbus-5

Electrically Scanning Microwave Radiometer, which operated at 19.35 GHz. The spatial resolution of the atlas maps is 1° lat × long. Despite the limitations of the SMMR instrument Rao felt able to conclude even at that early stage that '...in spite of various drawbacks, the microwave radiometer is at present indeed the best available means for estimating oceanic rainfall on a world-wide scale'.

Since then, the physical understanding of the relationships between hydrometeors in the atmosphere and microwave radiation measured by satellites has been further advanced particularly by Wu and Weinman (1984), through their studies of the effects of hydrometeor types, including aspherical ice, combined phase and liquid hydrometeors, and by Grody (1984), Spencer *et al.* (1983), and Spencer (1984) who pioneered the development of algorithms for passive microwave evaluation of rainfall over land as well as water, using higher-frequency data from the SMMR sensor on Nimbus-7.

The retrieval of rain over land, including land/sea mixed pixels, has proven more problematic than the retrieval of rain over water, primarily because the emissivity is generally high (and similar to that of precipitation), and very variable. However, despite many difficulties, even single passive microwave channel brightness temperatures may be used for rainfall identification over land, especially in the scattering region, if precipitation is relatively heavy. In these cases, especially at higher frequencies, some of the upwelling radiation stream from the surface is scattered by the precipitation, and a decrease in brightness temperature is observed by the satellite in the presence of rainfall. Spencer *et al.* (1983) suggested that, at 37 GHz, the scattering due to precipitation may be sufficient to lower the brightness temperatures to an asymptotic level of 230 K at 20 mm h^{-1}. Brightness temperatures as low as 163 K have been reported in extreme cases. However, perhaps the most useful approach so far to rainfall monitoring in the passive microwave over land has involved frequency differencing. The frequency algorithm of Grody (1984) uses two frequencies but like polarizations for rainfall-area delineation through the subtraction of the higher frequency brightness temperature from the lower frequency brightness temperature. Unfortunately, in general, such an approach can only be applied over land, although it is sometimes useful over water where heavy and very heavy rainfall is involved.

A second approach to rainfall monitoring over land involves the exploitation of polarization principles, through which radiation of a single frequency can be exploited, taking account of its horizontal and vertical polarization. It has been shown by Grody (1984) that, by using a proportion of each polarization, background characteristics can be subdued, even where these are complex, leaving attenuation by the atmosphere as the major influence on the signal. The polarization approach has been tested over both land and water. However, the consensus of opinion based on SMMR data analyses was that, over land, the use of polarization algorithms was less successful than that of frequency algorithms. Further, in the case of the polarization algorithms, the choice of rain/no-rain threshold was always subjective.

Recently, research in the RSUUB, supported by NOAA, the Meteorological Office, and the US Universities Space Research Association, has involved a combination of frequency and polarization approaches so that rain/no-rain boundaries might be established objectively for both frequency and polarization approaches, and so that radar might be used for rain/rain-rate calibration, and verification of results. In the RSUUB approach, a frequency algorithm and a polarization technique have been applied simultaneously over land. The purpose for this is two-fold: to generate rain areas and rain-rates for overland areas from the frequency algorithm, because SMMR-based research showed that 37–18 GHz frequency algorithms generally out-performed 37 GHz polarization algorithms over land; and second, to use the outputs from the frequency algorithm to help set objective rain/no-rain boundaries for the polarization technique, so that this technique could be used to produce realistic rain areas and rain-rates over neighbouring sea areas where the frequency approach is unrealistic.

Fig. 6 demonstrates the identified relationship between the brightness temperature difference of a frequency algorithm, and the polarization-corrected temperatures of a polarization algorithm for a test period in 1987. By projecting a line upwards from the zero point on the ordinate (line a) and calculating the best-fit regression through the distribution of points (line b), the rain/no-rain boundary of the polarization algorithm can be identified by the horizontal line c which passes through the point at which lines a and b intersect. Using this approach in relation to a large number of case-studies, verification statistics for satellite passive microwave versus radar rain/no-rain pixel classification have generally revealed a correspondence of about 95% (Barrett and Kidd 1989).

Figs 7(a) and 7(b) were produced for the evening of 15 October 1987 and the morning of 16 October 1987, respectively, using the combined frequency/polarization approach described above. Fig. 7(a) indicates heavy rain south-west of Cornwall with instantaneous rain rates as high as 64 to 128 mm h^{-1} on the eastern fringes, whilst over Spain even higher rainfall rates are indicated. By the morning of 16 October 1987 as shown by Fig. 7(b), when the centre of the Great Storm low-pressure system had crossed the United Kingdom to lie just off the Humber Estuary, the satellite detects an area of rain curving in an anticlockwise arc from the Scottish lowlands, across the Irish Sea and the Bristol Channel and into the Thames Valley. Another area of heavy rain is indicated off the east coast of Scotland with associated rainfall rates of up to 64 mm h^{-1}. In the centre of the North Sea, rain rates of up to 32 mm h^{-1} are observed.

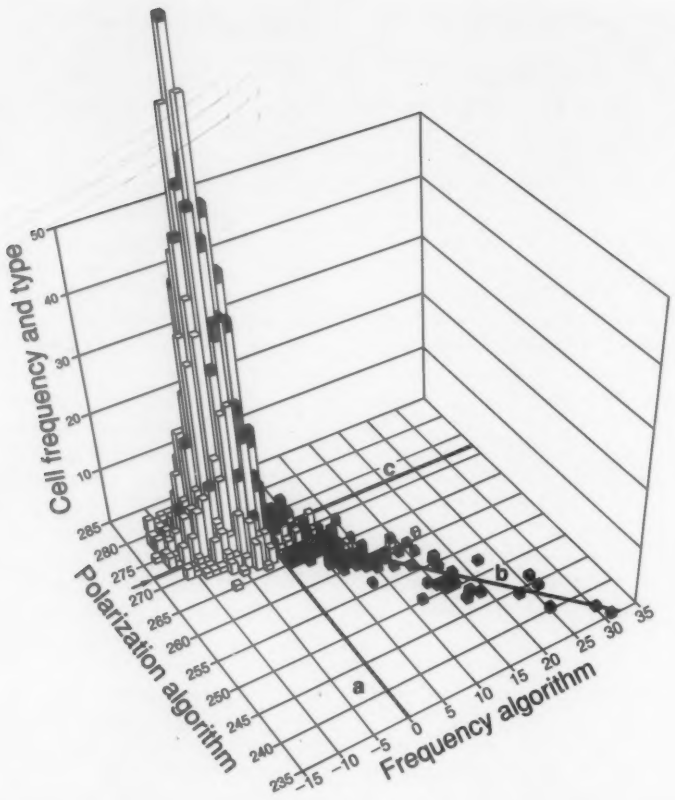

Figure 6. The basis of the Barrett and Kidd (1989) SSM/I rainfall algorithm — a plot of 85 GHz polarization versus 37–85 GHz frequency algorithm outputs to establish rain/no-rain boundaries objectively for both. Rainfall-rate data have been obtained from comparisons with FRONTIERS radar data. For further details see text.

Figs 7(c) and 7(d) show ground-based radar data from radars in the United Kingdom, Ireland, France and The Netherlands combined with Meteosat infra-red data at times corresponding to Figs 7(a) and (b). The success of the SSM/I algorithm in depicting the rain over France and elsewhere and especially beyond the limits of the radar coverage is evident.

Table II presents comparisons between FRONTIERS radar and microwave rain/no-rain pixels for this event in contingency table form. Since it has been demonstrated by Collier (1986) and many others, and confirmed for the present work by Barrett and Kidd (1989), that quantitative use of radar data is reasonably dependable up to a range of 100 km, and may be useful up to a range of about 140 km, but that beyond that limit only qualitative assessments of rainfall from the weather radar should be made, the data in Table II relate to a maximum range of 140 km from each radar location. Table II(a) shows results for the evening of 15 October 1987, when the R:R plus NR:NR (R=rain, NR=no rain) classifications were the same for 75% of all pixels within the areas of radar coverage. Table II(b) shows that, on the morning of 16 October 1987, the comparable result was lower, at 59% of all such pixels. Table II(c) shows that results for the entire period from 13 to 19 October 1987 yielded R:R and NR:NR correspondences on 80% of all occasions. It is interesting to note that the percentage correspondences on the morning of 16 October 1987 are the lowest yet obtained in any of the RSUUB SSM/I versus FRONTIERS radar studies. It is thought that the most likely reasons for this include the following.

(a) Temporal differences: Although the radar and satellite images have been obtained as close together in time as possible, small differences remain.

(b) Physical differences. The satellite, in observing a column of rain, does not, strictly speaking, yield an instantaneous rain rate but a rain rate related to circumstances prevailing over a period as long as 20 minutes in duration, dependent upon the depth of cloud and rate of fall of the hydrometeors.

(c) Disparities between the satellite and radar viewing geometry, i.e. the satellite receives radiation vertically, whereas the radar views rainfall more or less horizontally. The effect of this factor may have been particularly strong in the case of the Great Storm because of the influence of the exceptionally strong winds on the falling hydrometeors.

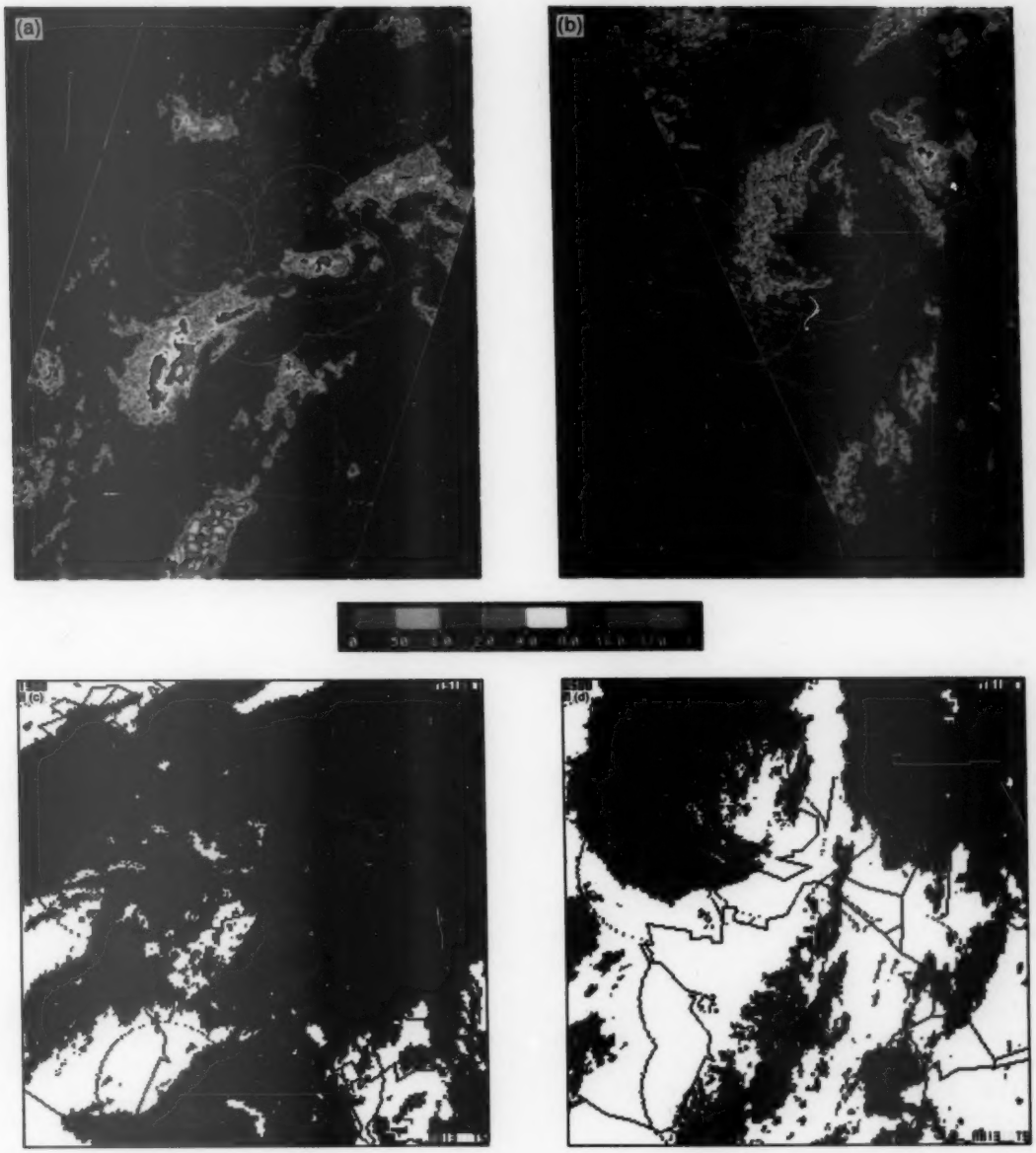

Figure 7. SSM/I-derived rainfall distribution on (a) 15 October at approximately 1900 UTC, and (b) 16 October at approximately 0500 UTC using the Barrett and Kidd (1989) algorithm. Rainfall rates (mm h^{-1}) are shown by the adjacent scale. Circles over southern Britain are drawn at 210 km radii from FRONTIERS radars. The combined Meteosat infra-red and ground-based radar image derived as part of the COST-73 Project (Collier *et al.* 1988) at (c) 1900 UTC on 15 October, and (d) 0500 UTC on 16 October. Radar data from the United Kingdom, Irish Republic, France and The Netherlands are used. Colours indicate — cloud temperatures; cyan −15 °C to −45 °C and blue < −45 °C: and rainfall intensities; magenta 0.3 to 1 mm h^{-1}, green 1 to 3 mm h^{-1}, yellow 3 to 10 mm h^{-1}, red 10 to 30 mm h^{-1} and black >30 mm h^{-1}. Coastlines and country boundaries are shown black. Also shown is the limit of the radar coverage (circles and rectangular frames). The projection of (c) and (d) is polar stereographic and each pixel is approximately 5 × 5 km.

5. Conclusions and recommendations

The satellite rainfall analyses presented in this paper follow earlier studies in the British Isles region using FRONTIERS radar data to calibrate the SSM/I rainfall algorithm, but the satellite wind-speed analyses have been prepared using a general model which, to our knowledge, has not yet been verified or calibrated in such northerly mid-latitudes. However, both the rain and wind-speed results reported above seem to confirm that the SSM/I instrument has clear potential for the monitoring of both rainfall and surface wind speeds in the British Isles region, especially over water, and,

Table II. Contingency tables (Rain (R), No Rain (NR)) for FRONTIERS radar/satellite SSM/I intercomparions for the polarization algorithms over water plus coasts (left-hand side), and the frequency algorithm over land (right-hand side) within 100 km of each radar site for (a) the evening of 15 October, (b) the morning of 16 October, and (c) the period 13–19 October 1987 (from Barrett and Kidd 1989).

(a)

Radar \ Microwave	R	NR	Total
R	274	263	537
NR	208	1681	1889
Total	482	1944	2426

Radar \ Microwave	R	NR	Total
R	59	342	401
NR	17	551	568
Total	76	893	969

(b)

Radar \ Microwave	R	NR	Total
R	207	68	275
NR	634	869	1503
Total	841	937	1778

Radar \ Microwave	R	NR	Total
R	49	389	438
NR	25	488	513
Total	74	877	951

(c)

Radar \ Microwave	R	NR	Total
R	2595	1417	4012
NR	3281	17478	20759
Total	5876	18895	24771

Radar \ Microwave	R	NR	Total
R	312	2256	2568
NR	105	7791	7896
Total	417	10047	10464

therefore, for improving weather forecasts not least in times of extremes.

We hope the future will see a continuation of the SSM/I north-west European rainfall monitoring programme currently centred in the RSUUB through our participation in the NASA WetNet project, and with support from NOAA and the Meteorological Office, and that a British Isles region-specific wind-speed evaluation and calibration programme will be commenced as soon as possible. SSM/I and SSM/I-type data are expected to become available for near-real-time forecasting purposes in the United Kingdom within 3 years. It is important to refine the more useful algorithms based on such data before then, so that they will be able to play their parts in improving forecasts, and investigating the impacts, of severe rain and wind storms as early as possible.

Acknowledgements

The authors wish to thank all their colleagues in the United Kingdom and USA who have helped in the preparation of this paper either through discussions or provision of data. Special thanks for one or both of such types of help are due to Drs D.B. Miller, P.K. Rao, J. Alishouse, R. Scofield and J. Wilkerson of NOAA/NESDIS, Washington DC; Drs R. Spencer and M. Goodman of NASA's Marshall Space Flight Center, Huntsville, Alabama; Dr R.C. Savage of Hughes Aircraft Company, F. Wentz of Remote Sensing Systems, Santa Barbara, California, and R. Brown and G. Shutts of the Meteorological Office.

References

Bailey, J.O., Barrett, E.C. and Kidd, C., 1986: Satellite passive microwave imagery and its potential for rainfall estimation over land. *J Br Interplanet Soc*, **39**, 527–534.

Barrett, E.C. and Kidd, C., 1989: Rainfall monitoring by the SSM/I with special reference to light rain over parts of north-west Europe. Final report (Stage I) to the Universities Space Research Association, Columbia, Maryland. University of Bristol, Remote Sensing Unit.

Barrett, E.C., Kidd, C. and Bailey, J.O., 1988: The Special Sensor Microwave Imager: a new instrument with rainfall monitoring potential. *Int J Remote Sensing*, **9**, 1943–1950.

Barrett, E.C. and Martin, D.W., 1981: The use of satellite data in rainfall monitoring. London, Academic Press.

Cardone, U.J., 1969: Specification of the wind field distribution in the marine boundary layer for wave forecasting. New York University, Geophysical Science Laboratory, Report No. 69-1.

Collier, C.G., 1986: Accuracy of rainfall estimates by radar. Part I: Calibration by telemetering raingauges. *J Hydrol*, **83**, 207–223.

Collier, C.G., Fair, C.A. and Newsome, D.H., 1988: International weather-radar networking in western Europe. *Bull Am Meteorol Soc*, **69**, 16–21.

Grody, N.G., 1984: Precipitation monitoring over land from satellite using microwave radiometry. *In* Proceedings of the International Geoscience and Remote Sensing Symposium (IGARSS 1984), Strasbourg 27–30 August 1984. Strasbourg, European Space Agency, No. ESA SP-215.

Hollinger, J., Lo, R., Poe, G., Savage, R. and Pearce, J., 1987: Special sensor microwave/imager user's guide. Washington DC, Naval Research Laboratory.

Kidd, C., Barrett, E.C., Bailey, J.O. and Palmer, H., 1989: The use of SSM/I imagery for rainfall monitoring, with special reference to the UK and surrounding seas. *In* Remote sensing for operational applications. Proceedings of the 15th Annual conference of the Remote Sensing Society, Bristol, 13–15 September 1989. University of Bristol, Remote Sensing Unit.

Munn, R.E. (ed), 1978: IUCRM colloquium on radio oceanography. *Boundary Layer Meteorol*, **13**, 1–429.

Nordberg, W., Conway, J., Ross. D. and Wilheit, T., 1971: Measurement of microwave emissions from a foam-covered wind-driven sea. *J Atmos Sci*, **28**, 429–435.

Rao, M.S.V., 1984: Retrieval of worldwide precipitation and allied parameters from satellite microwave observations. *Adv Geophys*, **26**, 237–336.
Rao, M.S.V., Abbott, W.V. and Theon, J.S., 1976: Satellite-derived global oceanic rainfall atlas (1973 and 1974). Washington DC, NASA, No. NASA SP-410.
Savage, R.C., 1978: The radiative properties of hydrometeors at microwave frequencies. *J Appl Meteorol*, **17**, 904–911.
Spencer, R.W., 1984: Satellite passive microwave rain rate measurement over croplands during spring, summer and fall. *J Clim Appl Meteorol*, **23**, 1553–1562.
Spencer, R.W., Olsen, W.S., Martin, D.W., Weinman, J.A. and Sartek, D.A., 1983: Heavy thunderstorms observed over land by the Nimbus-7 scanning multichannel microwave radiometer. *J Clim Appl Meteorol*, **22**, 1041–1046.
Swift, C.T. (ed), 1977: Special joint issue on radio oceanography. *IEEE J Oceanic Eng*, **OE2**, 1–159.
Wentz, F.J., 1988: User's manual, SSM/I Ocean products tapes. RSS Technical Report 033088. Santa Barbara, Remote Sensing Systems.
Wentz, F.J., Mattox, L.A. and Peteherych, S., 1986: New algorithms for microwave measurement of ocean winds: Applications to SEASAT and the Special Sensor Microwave Imager. *J Geophys Res*, **91**, 2289–2307.
Wilheit, T.T., Chang, A.T.C., Rao, M.S.V., Rodgers, E.B. and Theon, J.S., 1977: A satellite technique for quantitatively mapping rainfall rates over the oceans. *J Appl Meteorol*, **16**, 551–559.
Wu, R. and Weinman, J.A., 1984: Microwave radiances from precipitating clouds containing aspherical ice, combining phase and liquid hydrometeors. *J Geophys Res*, **89**, 7170–7178.

551.578.45(430.1):551.578.46:551.515

A heavy mesoscale snowfall event in northern Germany

W.S. Pike
19 Inholmes Common, Woodlands St. Mary, Newbury, Berkshire RG16 7SX

Summary

The geographical extent and particular causes of localized heavy snowfalls which occurred near south-west Baltic Sea coasts on the night of 11/12 January 1987 are investigated. The roles of convergence lines, coastal fronts, stationary 'warm cyclones' and eddy vortices are discussed.

1. Introduction

While heavy coastal snowfall was occurring in south-east England (Pike 1990a), a similar mesoscale event affected a narrow belt of Mecklenburg and Schleswig-Holstein in northern Germany. By 0600 UTC on 12 January 1987 a maximum 24-hour accumulation of 70 cm was reported from the Nusse area, some 30 km east-north-east of Hamburg.

2. The synoptic situation

Fig. 1 shows an extremely cold east to north-easterly airstream at 1200 UTC on 11 January 1987 over the Baltic Sea and surrounding land areas, between a strong anticyclone centred over Norway and a major low pressure complex centred well to the south between Corsica and Italy. A shallow thermal depression had formed over the Oder Bight, probably a similar development to that described in Pike (1990a) as occurring over the southern North Sea.

Tiesel (1984) identifies stationary depressions over sea areas adjacent to eastern Germany as 'Baltic heat cyclones'. Their formation occurs over the relatively warm water of the Mecklenburg and/or Oder Bights, whose coastlines these depressions tend to model themselves on. Tiesel explains their cyclogenesis as taking place during the calming phase after cold air penetration has occurred, which itself causes the weakness by means of stronger night-time cooling.

While the greatest weather activity may be expected when maximum thermal contrast exists between land and sea surfaces during hours of darkness, the depression can exist in a shallow and less-active form throughout the day, only completely losing identity when overwhelmed by synoptic-scale events, such as cloud spreading over or a stronger gradient/wind-field prevailing.

3. Satellite picture analysis

Fig. 2 is an AVHRR infra-red satellite image of the Baltic Sea area taken at 1236 UTC on 11 January by the NOAA-9 satellite. It gives a good general picture of the cloud patterns associated with the synoptic situation in Fig. 1, with any influence of major upper-cloud shields excluded to the south, we can form a very good impression of the wind direction prevailing in the lower troposphere. Here, given favourable conditions, streets of convective cloud (identified by Miura (1986) as requiring a certain wind increase with height*) parallel to the wind are forming almost immediately as the extremely cold arctic continental air advects from over land or ice surfaces out over the relatively warm Baltic

* Longitudinal rolls are realized when vertical wind shear (based on the wind difference between 1000 mb and the inversion base) is between 10^{-3} and 10^{-2} s^{-1}, and open cells are realized when it is smaller.

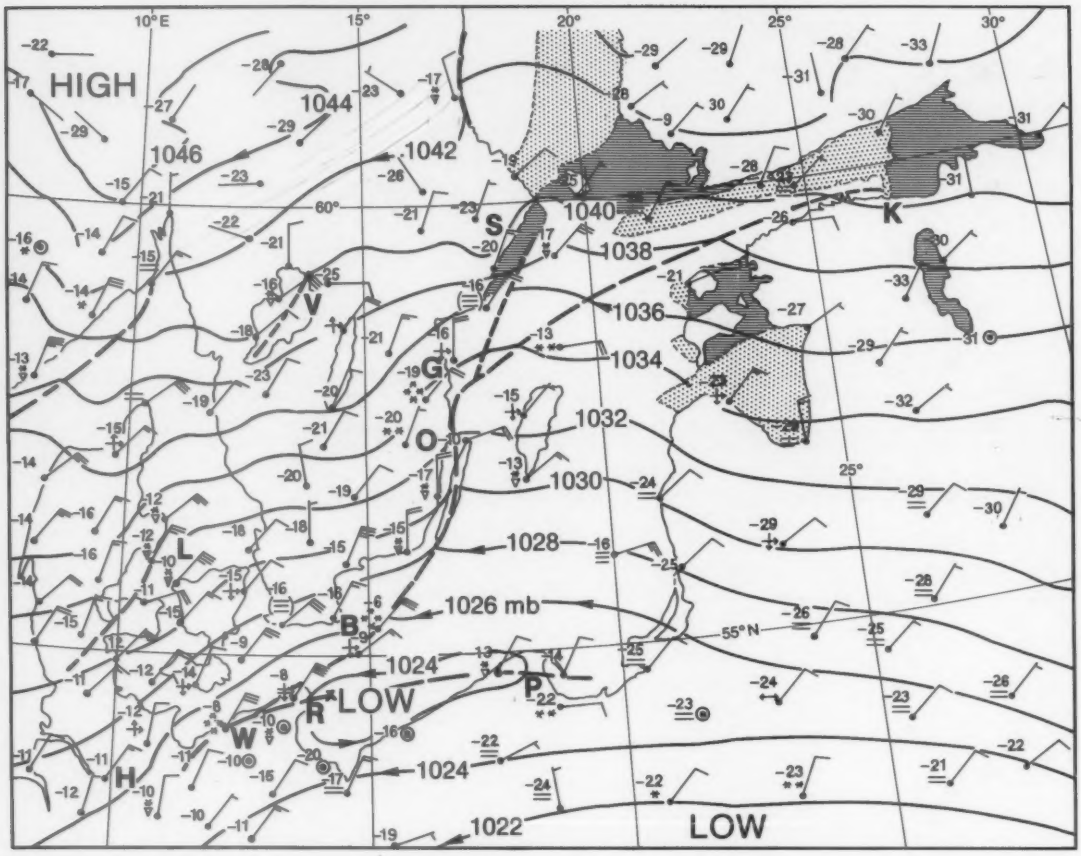

Figure 1. Surface synoptic chart for the southern Baltic and surrounding land areas at 1200 UTC on 11 January 1987. Heavy dashed lines indicate low-level convergence lines or coastal fronts, and letters indicate locations mentioned in the text. Shaded areas denote older ice areas and stippled areas denote young ice.

Sea and other areas of water. At first shallow and low, these cumuliform clouds eventually develop tops to 10 000–15 000 ft (see also Scorer (1986) chapter 6).

At this time, a pool of extremely cold air (temperatures at or below −20 °C at 850 mb, and −30 °C at 700 mb) was centred over southern Sweden and moving south-westwards (see chart in Kresling 1987a). The southern Baltic had surface temperatures of between 0 °C and 4 °C, hence great instability at low levels. Close inspection of Fig. 2 reveals cloud streets beginning to form over areas of young ice to the west and south of Finland.

Evidence of convergence can soon be seen, characterized by more prominent long plumes of cloud, such as that originating from near the older ice edge in the Gulf of Finland, just north-east of Kunda (K in Figs 1 and 2) in Estonia and running south-westwards, indicative of a major convergence line between the north-easterly airstream over Finland and the general east-north-easterly flow prevailing over most of the Baltic Sea further south. This persistent plume (it was in evidence in much the same location throughout the 12th) merges with another shorter one originating at the ice edge just east of Stockholm (S), and the two combine to produce much snow on the Swedish coast in the Gladhammar-Västervik region (G).

The convergence continues down the Swedish coast where the over-water flow meets a northerly land breeze, but some cells do travel 20–30 km inland in the Oskarshamn (O) area where the coastline is more nearly at right angles with the onshore wind, and the sheltering effect of Gotland causes a change in pattern. Further south the convergence plume curves south-westwards over Bornholm (B) towards Warnemünde (W) on the north German coast. Here again there are clear signs of merging convergence plumes, with another well marked line of cloud forming between near gale force east-north-easterlies over the Baltic and near-calm, clear conditions to the south, running from northern Poland (P) over Rügen (R) and then merging towards Warnemünde. Showing up more clearly in Fig. 3 (the AVHRR visible picture which covers the western section of Fig. 2) is the cloud formation resembling a ship's wake in the lee of Rügen Island. Here, the steep

Photograph by courtesy of University of Dundee

Figure 2. NOAA-9 AVHRR infra-red satellite picture at 1236 UTC on 11 January 1987. See text for locations indicated by letters.

cliffs rise to 100–150 m AMSL in the Stubbenkammer–Konigsstuhl area of the north-east coast.

Fig. 3 also shows close proximity of the cirrus shield in the extreme south, as well as giving an enlarged view of a genuine lake convergence effect of cloud streets over Lake Vänern (V) which remains unfrozen. Convective cells moving inland near Oskarshamn (O) appear to converge into two brightly illuminated streets, suggesting uplift produced by land-breeze near the coast. A similar effect occurs at the eastern Danish coast around 55½° N, 10° E. Medium-level wave-cloud is just visible in the top right corner of this picture over central Sweden, forming at right angles to the wind direction.

The shield of upper cloud moved north-north-eastwards to cover areas south-east of a line from Oskarshamn to Rügen by 0230 UTC on the 12th (in NOAA-9 composite from *Das Europaeische Wetterbild* — not shown), and Fig. 4 shows that the upper cirrus had, by 1224 UTC, moved further westwards, to lie from central Denmark to the Dutch border. This picture marks the temporary end of significant coastal-front activity in the south where upper-cloud and synoptic-scale features overwhelm radiation effects. However, further north, the Kunda to Gladhammar convergence line is still in evidence, although the strong east-north-easterlies have swept inland over south-eastern Sweden behind an active, warm coastal front.

Nevertheless, the 'lumpy' nature of the cloud tops over East Germany in Fig. 4 does indicate that Baltic warming of the strong north-easterly airstream was producing much activity from embedded cumulus and cumulonimbus which were being swept southwards inland, within the general background of thick upper and medium frontal cloud layers.

4. Discussion of the snowfalls

With 40–50 cm of snow already lying in south-east Sweden, coastal accumulations over the period 9–14 January 1987 during the cold outbreak tended to increase gradually by 5–15 cm per day until some stations reported approximately 90 cm (nearly 3 ft) lying, e.g. at Oskarshamn and Krokshult by 0600 UTC on the 12th, then at Gladhammar-Västervik and Herrvik by 0600 UTC on the 14th, when Oskarshamn measured a maximum reported value of 105 cm, an increment of 50 cm since the north-easterlies began on the 9th. Gladhammar registered a maximum 24-hour fall of 23 cm up to 0600 UTC on the 12th, and this was the period when spectacular snowfalls occurred further south in Germany.

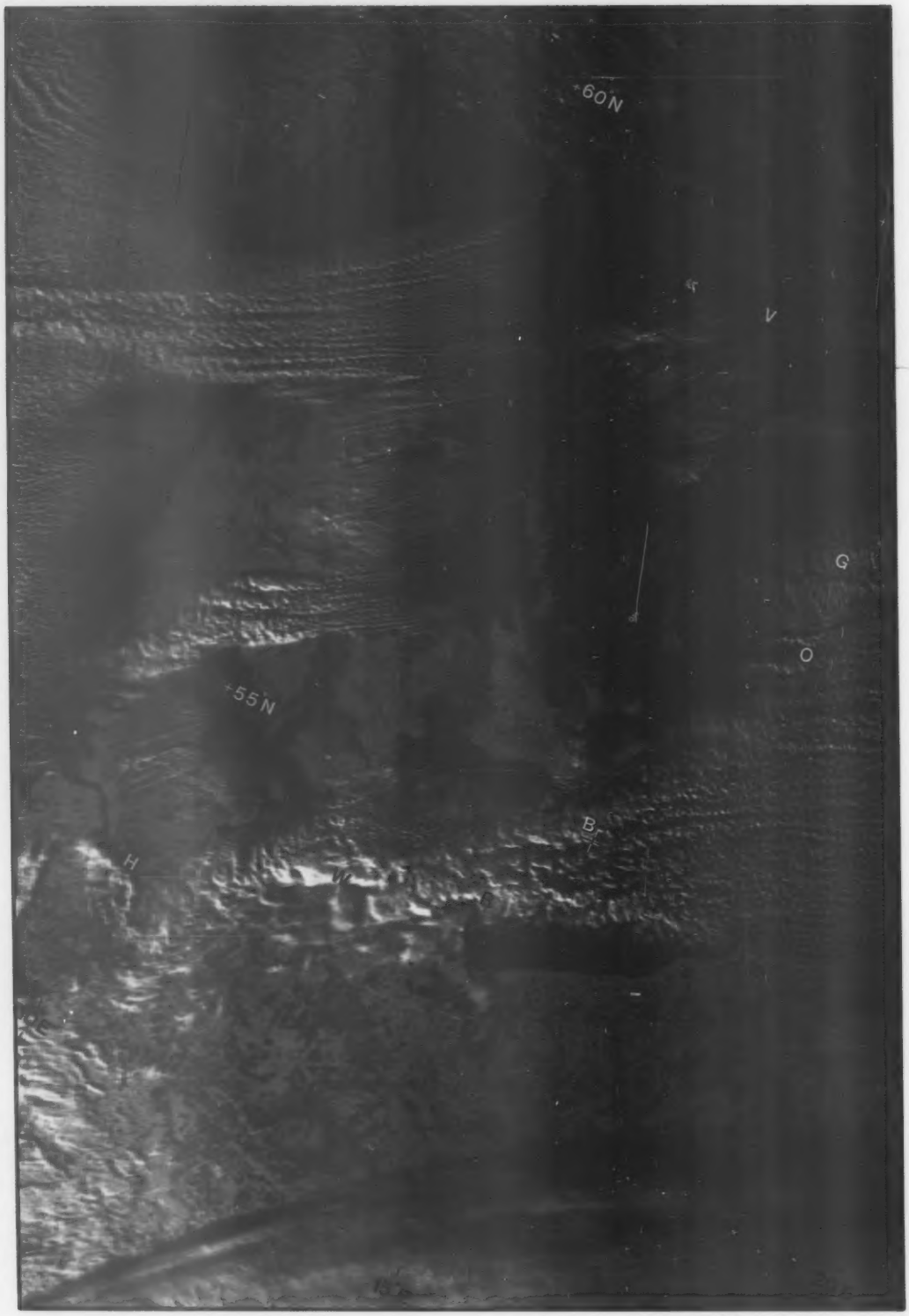

Photograph by courtesy of University of Dundee

Figure 3. NOAA-9 AVHRR visible imagery satellite picture at 1236 UTC on 11 January 1987, corresponding to Fig. 2.

Fig. 5 gives the distribution of new snowfall recorded in the 24-hours up to 0600 UTC on 12 January 1987 in northern Germany. The heaviest accumulations occurred in a long, narrow belt stretching from Warnemünde to near south-east Hamburg. A secondary wedge-shaped area stretches from just north of Greifswald towards Teterow, with a thin division where negligible snow fell between these two areas. In extreme south-east Schleswig-Holstein, several locations to the north-east of Hamburg (e.g. Trittau and Ratzeburg) recorded 40–50 cm, with a maximum fall of 70 cm reported from the Nusse area.

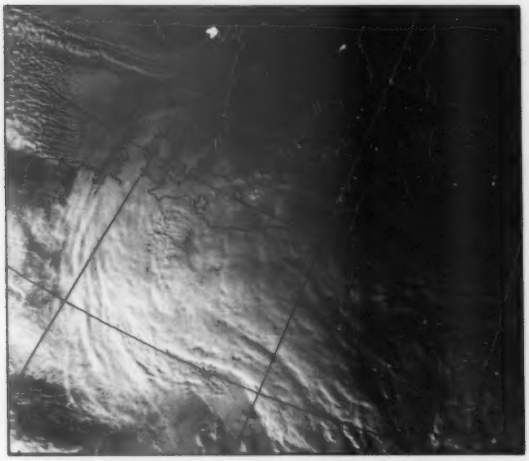

Photograph by courtesy of University of Dundee

Figure 4. NOAA-9 AVHRR visible imagery satellite picture at 1224 UTC on 12 January 1987.

At Bergedorf (a south-east suburb of Hamburg) reliable observations of the snowfall indicate that, with only few interruptions, it continued from 1500 UTC on the 11th until about 0630 UTC next morning. The most intense snowfall, accumulating at a rate of 7 cm h^{-1}, occurred on the evening of the 11th between 1900 and 2115 UTC as the cold pool centre was, by extrapolation, passing overhead (see Kresling 1987a).

This 16-hour period of snow produced a total of 30–50 cm in the Bergedorf area. One station measured a water equivalent of 23.4 mm from 37 cm of fresh snow, which gives a ratio near 1:15 in the very cold conditions, temperatures during the snowfall rising from around −12 to −10 °C in that time-span. Given similar water equivalents to those recorded in the United Kingdom, the higher rainfall to snow depth ratios (than the 1:11 or 1:12 experienced in England) may explain why maximum snow depths in colder German conditions yielded 10–20 cm more snow on the ground (temperatures were nearer −5 to −8 °C in south-east England, see Pike 1990a).

Wright (1987) mentions similar problems occurring on the local German suburban railway lines (conductor rail) to those experienced in north-west Kent, also due to heavy snow that Sunday evening (11th). Fig. 6 gives a visual indication of snow depths that affected Rhinebeck, 2–3 miles north-east of Bergedorf. Some cars were still almost buried by snow a week later, although the German legal requirement that domestic front paths are to be kept clear of fresh snow accumulations resulted in much activity during the 11th and 12th for local townspeople.

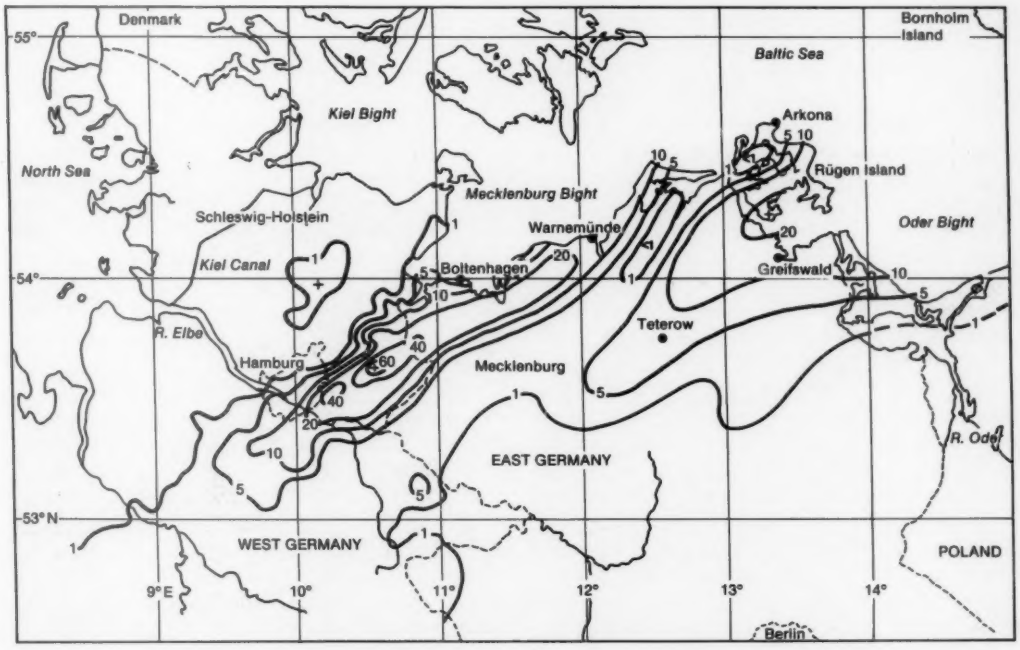

Figure 5. New snowfall (cm) in northern Germany in the 24 hours up to 0600 UTC on 12 January 1987.

Photograph by courtesy of P.B. Wright

Figure 6. A suburb of Hamburg after the snowfall of 11/12 January 1987.

5. Mesoscale analysis

The general synoptic situation over northern Germany, as described in section 2, appears similar to that of 9 February 1956, outlined in Tiesel (1984). In both cases a stationary warm cyclone lay over the Oder Bight. An unstable boundary line was formed between streams of air moving at very different speeds, characterized by a Beaufort Force 8–9 north-easterly wind at Arkona Lighthouse (on the northern tip of Rügen Island) and a near-calm at Greifswald, some 66 km to the south.

From 0000 UTC on the 11th to 0000 UTC on 12 January 1987, radiosonde ascents from Greifswald showed the air to be extremely cold, moist and unstable to sea temperatures up to about 650 mb (12 000 ft). They featured a north-easterly wind which was increasing with time and height in this layer, and such conditions of wind shear are thought to be very conducive to the formation of streets of cumuliform cloud, as seen in Fig. 2 (Miura 1986, Scorer 1986).

By 2100 UTC on the 11th (Fig. 7), a pronounced coastal front had developed along the Mecklenburg Bight coast, primarily due to the coldest air passing overhead at that time and also radiation cooling over snow covered ground providing a near −20 °C thermal contrast across the boundary (convergence) line, with Baltic Sea-surface temperatures remaining in the range 0 to 4 °C.

Marked by convergence and convection forming a procession of heavy snow showers (as shown by radar study in Pike (1990b), and in Kresling (1987b)), the unstable boundary line/coastal front produced many small lateral oscillations. A few of these developed into eddy vortices which either became detached from the stationary warm cyclones over the sea, or else were shed downwind of an island or promontory (see the detailed study in Walter 1989). One suspects that areas of water just downwind from Bornholm or Rügen are two such preferred sites for formation of eddy vortices off north-east Germany in cold north-easterly airstreams. Although spacing of synoptic stations does not permit mesoscale analysis, one small eddy vortex appears to have produced heavy snow in passing close to Arkona soon after 1400 UTC on the 11th, and this affected Warnemünde between 1600 and 1700 UTC. Tiesel (1984, pp. 360/1) describes detached eddy vortices being shed south-westwards from the stationary Oder Bight warm cyclone on 9 February 1956. Generally speaking, one may expect them to travel downstream along the boundary line at a speed intermediate between low-level airflows on either side of the discontinuity (after Tricker 1964, pp. 179–180). The German term for eddy vortex is *randwirbel*, which is used by Tiesel to describe the 1956 case.

Formation of a small, marine, warm cyclone was noted further east at 2100 UTC on 10th January, some 40 km north-west of Gdynia, off the Polish coast (personal correspondence with Dr R. Tiesel), with timing of development (and that of subsequent similar warm cyclones) strongly suggesting that they are likely to appear just as the pool of coldest upper air is approaching.

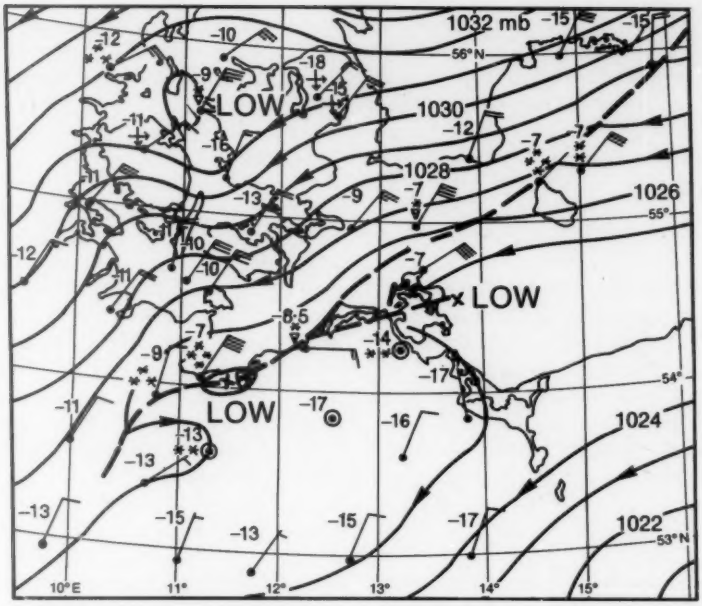

Figure 7. Surface synoptic chart for northern Germany at 2100 UTC on 11 January 1987, with isobars drawn at 1 mb intervals. Heavy dashed lines indicate position of low-level convergence lines/coastal fronts.

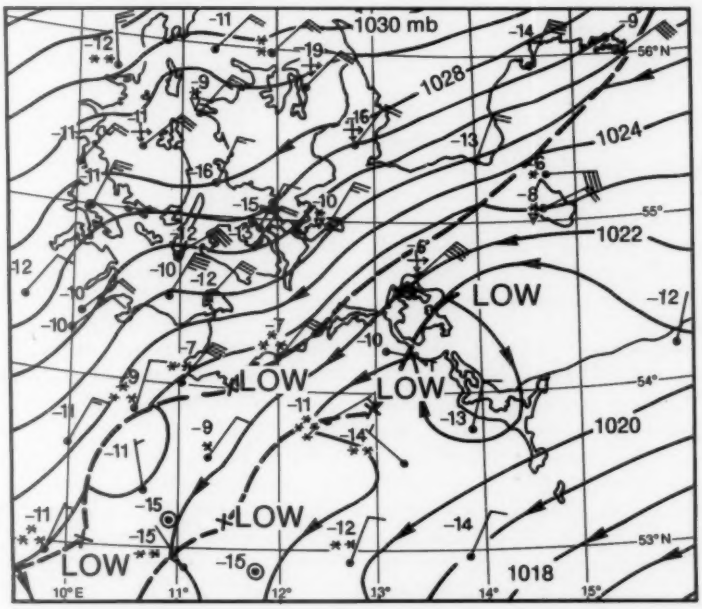

Figure 8. As Fig. 7 but for 0600 UTC on 12 January 1987.

However, on 11 January 1987 a small stationary mesoscale heat-low appears to have developed intermittently *in situ* on the marked coastal front over the Mecklenburg Bight between Warnemünde and Boltenhagen from just before 1400 UTC, with this showing up well in Fig. 7 when weather activity was intense. Fig. 8 suggests a meso-low is still in evidence at 0600 UTC the next morning, although it is fading fast beneath increasing cloud and strengthening gradient wind. It appears to be a stationary eddy-vortex type of development, forming near the coast at the edge of the very strong north-easterly airflow over the sea, and plays an important part in maintaining heavy precipitation along a narrow belt downwind.

Such *in situ* developments of small vortices, particularly when they happen to occur in a favoured area nearby and just downstream of a particular coastal station, would explain the surface wind veering rather than backing there as the land-breeze sets in (see Weybourne and Wainfleet AWS observations in Pike (1990a)). Two similar events which are believed to have occurred in association with the intermittent development over the southern Mecklenburg Bight are in evidence from the Warnemünde anemograph trace (not shown); the first occurring between 1400 and 1600 UTC, and the second is demonstrated by reproduced surface observations (Fig. 9) during the night of the 11th/12th. This shows what may be interpreted as a temporary oscillation of the coastal front out to sea, with a distinct land-breeze regime lowering temperatures by an average of 1 °C h^{-1} during a 4-hour period, during which the surface wind was southerly or calm between 2230 and 0010 UTC, then being immediately replaced again by the strong north-easterly wind with rapid recovery of temperature by 0100 UTC on the 12th.

It appears that several mesoscale eddy vortices moved inland from the Mecklenburg Bight towards south-east Hamburg, occasionally intensifying the overnight snow along a narrow belt where the coastal front extended over part of Schleswig-Holstein. These developments appear to have had a similar effect to the small eddy-vortex over Lincolnshire, described in Pike (1990a), which also gave heavy snow over a small area. The features behave as mesoscale, shallow polar-lows in (a) forming over the sea, (b) continuing over the coast then (c) decelerating and filling up over land.

The distribution of snow in Fig. 5 appears to have been due to a series of small eddy disturbances passing south-westwards from the stationary Oder Bight warm cyclone, this process beginning towards midnight, with Greifswald reporting continuous moderate snow throughout the night from 2300 UTC on the 11th.

This process extended a second coastal front south-westwards from the Rügen area, as indicated in Fig. 8, during the latter part of the night, and this analysis in part explains the distinct gap between the two snow areas in Fig. 5. The satellite pictures suggest a second factor was involved, associated with the ship's-wake cloud pattern in the lee of Rügen Island, from which one suspects that subsidence would have earlier been affecting a short length of the coastal front along the north German coastline, damping its shower activity there (see Scorer 1986, chapter 9).

6. Conclusions

The east-north-east to west-south-west orientation of the coastline along the Mecklenburg Bight (south side) presented a shallow angle to the onshore wind which was an extremely favourable situation to permit continuing coastal convergence and uplift between (a) a strong, moist, showery north-easterly airflow over the sea, with the air temperatures typically −6 to −10 °C, and (b) stagnating, colder overland air near −20 °C. A well marked coastal front formed between the two airflows.

During the hours of darkness overnight 11/12 January 1987, while thermal contrast between the airflows was greatest, a heavy snowfall of between 20 and 70 cm occurred in a 16-hour period along a narrow, sharply defined belt which was, geographically speaking, an extension of the southern Mecklenburg Bight coastline downwind to the west-south-west towards south-eastern Hamburg.

The formation of small Baltic Sea warm cyclones forming first over the Oder Bight and later over the Mecklenburg Bight in the extreme south, intensified the snowfall from time to time in association with smaller eddy-vortices which were shed south-westwards, extending eventually two coastal fronts; one from Warnemünde to south-east Hamburg and another from Rügen towards Teterow.

The steep cliffs of Rügen Island also provide a natural topographic division of a cold north-easterly airstream, downwind of which the coastal convergence line (or often a more developed coastal front) is likely to form along a marked boundary between fast- and slow-flowing airstreams at low levels.

The case of 11/12 January 1987 was similar to that producing 20–50 cm of fresh snow at a similar local time in coastal areas of south-east England and East Anglia (Pike 1990a). However, accumulations 10–20 cm deeper in northern Germany were most probably the result of 'water-equivalent to snow-depth ratios' nearer 1:15 in the colder conditions, as opposed to the 1:11 or 1:12 experienced simultaneously in England. Water yields from snowfalls were comparable (generally between 22 and 32 mm) in both countries.

While the formation of a marine warm cyclone is occurring *in situ* nearby, and especially when this occurs immediately downstream of a particular coastal station, a temporary veering of the surface wind is likely to occur as the land-breeze sets in. Heavy and prolonged showers tend to accompany these changes of wind direction, but often affect only a limited and narrow belt (25–30 km wide) near the coast.

Both Figs 7 and 8 confirm that analysis of surface synoptic charts with isobars drawn at 4 or 5 mb intervals is too coarse to depict the small mesoscale heat cyclones and eddy vortices which are more readily observed with isobars spaced at 1 or 2 mb intervals.

Acknowledgements

At Bracknell, to Meteorological Office staff: G.A. Monk of the Nowcasting and Satellite Applications Branch for discussions and extra satellite data. Also to L. Rowley for accessing the data bank's surface- and upper-air information to allow Figs 1, 7 and 8 to be drawn and conclusions made. Baltic Sea ship observations were kindly sent by R. Whyman of the Marine Advisory and Consultancy Service. Further data was obtained courtesy of helpful staff in the Library and Archives.

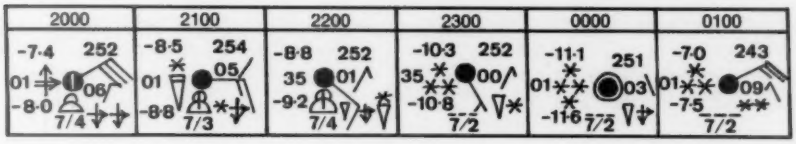

Figure 9. Sequential synoptic observations for Warnemünde from 2000 UTC on 11 January to 0100 UTC on 12 January 1987.

Much useful co-operation came from A. Kresling in the Deutschen Wetterdienst Seewetteramt at Hamburg, including early morning satellite data for Eastern Europe*, snowfall information over West Germany (upon which half of Fig. 5 is based), some extra synoptic observations from German shipping in the Baltic Sea, and water equivalents of snowfall at Hamburg-Bergedorf. The other half of Fig. 5 is based on information supplied by the Met. Dienst der DDR: from Dr Kolbig in the Climatological Headquarters (Hauptamt fur Klimatologie), Potsdam and Drs Holz and Tiesel at the Rostock-Warnemünde Meteorological Office.

The paper by Tiesel (1984) was sent by Prof. Dr Manfred Geb of the Meteorological Institute, Free University of Berlin (and further information was sent by Dr Tiesel later). Photographs (of which Fig. 6 is one) and helpful correspondence came from Dr Peter Wright, who was then at the Max-Planck Institute for Meteorology in Hamburg during the 1987 snowfall.

Snowall data from stations in south-east Sweden came from S. Larsson-McCann at the SMHI Climat Division, Norrköping.

References

Kresling, A., 1987a: Die starken schneefälle östlich Hamburgs vom 11 auf den 12 Januar 1987. *Wetterkarte des Deutschen Wetterdienstes.* Nr. 11, Freitag, den 16 Januar 1987.

—, 1987b: *Wetterkarte des Deutschen Wetterdienstes.* Nr. 13, Dienstag, den 20 Januar 1987.

Miura, Y., 1986: Aspect ratios of longitudinal rolls and convection cells observed during cold air outbreaks. *J Atmos Sci*, **43**, 26–39.

Pike, W.S., 1990a: Persistent coastal convergence in a heavy snowfall event on the south-east coast of England. *Meteorol Mag*, **119**, 21–32.

—, 1990b: Radar study of the snowfall in south-west Cornwall on 12 January 1987. *Meteorol Mag*, **119**, 97–102.

Scorer, R.S., 1986: Cloud investigation by satellite. Chichester, Ellis Horwood.

Tiesel, R., 1984: Die Wärmezyklonen der westlichen und mittleren Ostsee. *Z Meteorol*, **34**, 354–365.

Tricker, R.A.R., 1964: Bores, breakers, waves and wakes. London, Mills and Boon.

Walter, B.A., 1989: A study of the planetary boundary layer over the polynya downwind of St. Lawrence Island in the Bering Sea using aircraft data. *Boundary Layer Meteorol*, **48**, 255–282.

Wright, P.B., 1987: German Weather Conditions. *Climatol Obs Link*, No. 201. p. 20.

* *Das Europaeische Wetterbild* — satellite composites (NOAA-9 AVHRR) issued by the Institute of Meteorology at the Free University of Berlin.

Reviews

Carbon dioxide and global change: earth in transition, by S.B. Idso. 150 mm × 220 mm, pp. viii+292, *illus*. Tempe, Arizona, IBR Press, 1989. Price $19.95.

Over the last decade, a general scientific consensus has developed that rising concentrations of the greenhouse gases in the atmosphere will lead to fundamental climatic changes, with severe impacts on our way of life. This consensus has received widespread publicity. But throughout this time Sherwood Idso, a research physicist with the Water Conservation Laboratory in Phoenix, Arizona, has maintained that we should welcome increases in atmospheric CO_2, since the results will be entirely beneficial for life on Earth. His articles on the subject have appeared in a wide range of journals. Now, the sum of his ideas is gathered between the covers of this book.

Idso takes as his starting point the variations in atmospheric CO_2 concentrations over the totality of the Earth's existence. As the luminosity of the Sun has increased, so atmospheric CO_2 concentrations have decreased, thus maintaining an approximate balance which has produced climatic conditions suitable for the development and sustenance of life. Present-day CO_2 concentrations are dangerously low for the maintenance of plant life, and therefore any process which augments their levels is to be welcomed. Idso then argues that the temperature increases predicted by general circulation models (GCMs) for an equivalent doubling of atmospheric CO_2 are gross exaggerations. He proposes, by comparison with conditions on Mars, Venus and the early Earth, an equivalent CO_2 doubling temperature increase of only 0.4 °C. Therefore, on the one hand increasing CO_2 concentrations will bring valuable direct effects to the biosphere whereas on the other hand the dramatic climatic changes suggested by modelling studies will simply not occur.

The book is divided into two main parts. The first is devoted to the climatic aspects of the greenhouse effect, and contains five sections. The first of these defines the problem in the context of the long-term history of the Earth. The second reviews the GCM modelling results for doubled CO_2 concentrations. Both sections are quite brief, taking together only 15 pages. We then move into the real 'meat' of the book. The third section is devoted to a strong criticism of GCMs. It should be noted, however, that these criticisms add nothing more to what is already openly admitted and debated by the modellers themselves. In the fourth section Idso then proceeds to present his empirical approach to the problem, outlined above, which yields a 0.4 °C warming for doubled CO_2. He further proposes that there may be a maximum limit to the greenhouse warming of the Earth of 38.5 °C (4.5 °C above the current figure) provided all else (planetary albedo, atmospheric pressure, etc.) remains constant. The first part of the book closes with a critical review of attempts to pin-point the signal of greenhouse warming through, for example, analysis of regionally averaged temperature series.

The second part of the book discusses the beneficial direct effects of increasing CO_2 concentrations on the biosphere. There are four sections dealing respectively with plant responses, the beneficial effects of high levels of atmospheric CO_2 on plants experiencing environmental stress, a review of studies which suggest that there are already signs of a CO_2-induced 'greening of the Earth', and the beneficial affects for animals. The book closes with a general review of the evidence that has been presented in the context of other environmental problems.

There is a clear change of pace between the first and second parts of the book, and Idso is clearly more at ease discussing the direct effects of CO_2 on the biosphere than he is with the indirect effects. Notwithstanding this point, the writing is clear and intelligible to the non-specialist reader. The production is camera-ready with few, but adequate, explanatory diagrams. One hundred of the 292 pages are devoted to the list of references, some 2700 in all. Idso is uncritical of those authors whose work supports his views. However, he devotes many pages of argument to undermine, for example, the Jones *et al.* temperature series which suggests a 0.5 °C global warming this century.

This is a biased book, devoted to the explanation and support of one man's ideas. Anyone buying it should be aware of this fact, and I would only recommend it either to those who wish to learn more about Idso's ideas, or to politicians seeking justification for their unwillingness to take action to limit emissions of the greenhouse gases. We must still await the much-needed publication of an objective and well-informed discussion of all the scientific points-of-view in the greenhouse debate.

J.P. Palutikof

Climatic atlas of the Indian Ocean. Part III: Upper-ocean structure, by S. Hastenrath and L.L. Greischar. 345 mm × 230 mm, pp. xxvi + 247 charts, *illus*. University of Wisconsin Press, 1989. Price $40.00.

For more than a decade the first two parts of this atlas series by Hastenrath and Lamb (1979) have been a useful reference on the surface climate and heat budget of the Indian Ocean. This third part, documenting the annual cycle of subsurface structure and the upper-ocean heat budget, is a welcome addition. It covers the same area on the same scale and in the same format at the first two volumes. However, the relative sparseness of subsurface observations makes some loss of resolution inevitable. In this volume the data are presented on a

2° latitude × longitude grid. Most of the material comes from the Master Oceanographic Observation Data Set (MOODS) compiled by the Fleet Numerical Oceanography Center, Monterey, California. In the area under consideration (The Indian Ocean to 30° S, 120° E) this comprised nearly 320 000 temperature soundings and 18 000 for salinity at the time when the atlas was made. The authors found it necessary to screen out more than one third of the temperature soundings, reducing the number used to less than 200 000. Of these, 88% were collected during 1963–84. In contrast, about 4.5 million sets of surface ship observations were used in compiling the first two volumes — from the TDF-11 data set for the years 1911–70.

About one third of this volume is devoted to monthly charts of temperature at seven levels: surface, 50, 100, 150, 200, 300, 400 m below sea level, contoured at 2 °C intervals. One can see fairly well the annual cycle of major features like the subtropical gyre and the zonal band of low temperature separating it from the equatorial counter-current, and their vertical structure. At the surface though, the extra resolution in the charts of Part I of the series allows smaller-scale phenomena such as the upwelling regions off Arabia and Somalia to be seen more clearly than here. Subsurface there are some intriguing features, for example at 100 m to the west of Sumatra. They could have some bearing on the development of the Indonesian warm pool and its relationship to the twice-yearly equatorial jet in the Indian Ocean. But are they real? One would like to look more closely at them.

Other thermal products include monthly charts of mixed-layer depth, base depth of the thermocline, thermocline intensity, heat storage (to 400 m) and oceanic heat export. The monthly and annual charts of 'net oceanic heat gain' in Part II of the series are reproduced here, reanalysed at 2° spatial resolution for convenient comparison. All the products shown in the atlas are clearly defined and briefly discussed in the 26 pages of introductory notes.

With so few observations available, salinities have been averaged into two 6-monthly periods (November–April and May–October) corresponding to the north-east and south-west monsoon seasons, and charts show the distributions at the surface, 100 m and 300 m. Despite the shortage of salinities, the authors offer monthly charts of geopotential anomaly at the sea surface relative to 400 decibars. They justify this by showing that, in five selected areas, the temperature–salinity relationship is sufficiently well defined to allow anomalies to be calculated directly from temperature profiles — with sufficient accuracy for the contour interval (10 dyn cm) adopted here. Monthly charts of surface currents and their divergences (regrettably not extending east of 100° E) are based on the archive of the Meteorological Office. Again, whilst the evolution of the major currents can be followed clearly, the scarcity of observations, particularly south of the Equator, makes one doubtful of the reality of some of the smaller features.

The atlas concludes with a set of selected vertical sections and temperature profiles. Very few errors were noticed — a few wrongly directed arrows in some of the charts of geopotential anomalies. What has been done is clearly defined. The limitations are on the sparseness of the data and their uneven distribution rather than in the treatment.

It is timely. Many more data have gone into this atlas than any previous one dealing with thermal properties in this region. It should be in any library with an interest in marine climate.

J.C. Swallow

Applications of weather radar systems — a guide to uses of radar data in meteorology and hydrology, by C.G. Collier. 170 mm × 246 mm, pp. 294, *illus*. Chichester, Ellis Horwood, 1989. Price £44.50.

Applications of radar technology in meteorology have been under development for over 40 years, and weather radars are now used in many countries for operational and research purposes. Chris Collier has been closely involved in the developments in the United Kingdom for many years, and this book reflects his wide experience of the subject. He currently leads a Branch of the Meteorological Office responsible for 'nowcasting' and satellite applications. This book, one of a series on remote sensing, is directed towards the practical applications of weather radars that can be used operationally, and provides information on techniques and an assessment of their success in a wide range of applications.

Following an account of the basic theory, which includes Doppler and multi-parameter radars, chapter 3 deals with precipitation measurement; later chapters discuss the role of satellites in this very important application and extend the subject into precipitation forecasting. Here we find some strange imbalances. For example, the choice of wavelength is dealt with in one paragraph, whilst the real-time calibration system developed by the author occupies over ten pages when this (excellent) work is fully covered in numerous published papers. The use of X-band radars for urban storm warning purposes, which featured prominently at the 1989 conference on Hydrological Applications of Weather Radar at the University of Salford, is also neglected. The chapter on satellite sensors for precipitation measurement (estimation would be a more suitable word) is succinct and well written, and is coupled with five colour plates illustrating the potential of using combined satellite and radar images for precipitation forecasting. Appropriately, short-period forecasting (chapter 6) receives extensive treatment,

covering methods of describing and tracking precipitation echoes, and the forecasting of severe storms, also looking forward to the possibilities for combining radar data with numerical forecasting models.

The logical development is flood forecasting using radar data; chapter 7 starts with some data on flood damage costs and potential savings in England and Wales, but contains little information of direct use on hydrological forecasting methods. It concludes that 'only if ways can be found for dealing with errors in radar estimates of precipitation, will radar attain its potential in hydrological forecasting'. Amen to that!

Weather radar networks now exist in quite a few countries and regions, so it is appropriate for this book to include a chapter on this topic, concentrating on the factors influencing network design. The section giving examples of networks is disappointing. The description of radar networking in the United Kingdom and the USA has a curious emphasis on the history of the developments, with no technical information on equipment, data, format, transmission speeds, etc. Japan, with perhaps the densest network in the world, receives scant mention.

Further applications dealt with in later chapters include the use of radar data to improve our knowledge of the frequency of extreme amounts of precipitation, depth-area-duration analysis for use in storm drainage design, and probable maximum precipitation estimation. These are undoubtedly areas where the full potential of radar data has still to be explored. The role of radar in studies of airborne pollutants is an important application, and its inclusion illustrates the breadth of coverage of this book. Illustrations of the rainfall over the United Kingdom during the passage of the Chernobyl plume and a map of the deposition of caesium-137 underline the contribution radar has to make in this field, which has grown rapidly in importance in the last few years. The concluding chapter outlines a number of uses of weather radars in furthering research into meteorological phenomena such as severe convective storms and hurricanes, and discusses some of the recent developments in radar technology including Doppler radars.

Overall, this book is notable for its breadth of coverage and the huge volume of scientific literature it has drawn on. There are no less than 780 references cited. The author's experience has enabled him to draw heavily on information from many parts of the world, which will give the book a strong international appeal. Typographical errors are relatively few for a book of this size and character. Its cost is not too excessive in these days and I have no doubt it will find a place on the shelves of some who work in this specialized field either in research or in an operational role, as well as being an important addition to the shelves of university libraries and research institutes as a major reference work.

V.K. Collinge

Books received

The listing of books under this heading does not preclude a review in the Meteorological Magazine at a later date.

The dynamics of the coupled atmosphere and ocean, edited by H. Charnock and S.G.H. Philander (London, The Royal Society, 1989) comprises papers presented at a Discussion Meeting in December 1988. They describe work being carried out on both regional and global models.

Compact data for navigation and astronomy for the years 1991–1995, by B.D. Yallop and C.Y. Hohenkerk (Cambridge University Press, 1990) aims to provide navigators and astronomers with simple, efficient methods for calculating the positions of heavenly bodies. It has been prepared by HM Nautical Almanac Office at the Royal Greenwich Observatory, Herstmonceux Castle.

Rainbows, halos, and glories, by R. Greenler (Cambridge University Press, 1989) is a paperback edition of the book which was originally published in 1980. It contains many illustrations of the various phenomena with explanations in non-technical language and ways of finding them.

Global environmental issues, by D.D. Kemp (London, New York, Routledge, 1990) analyses the role in global environmental issues of the greenhouse effect, acid rain, ozone depletion, drought and nuclear winter by way of the common thread of climatology. The author has sought the middle ground in discussing the complexity of the problems.

The earth's climate and variability of the sun over recent millenia, edited by J.-C. Pecker and S.K. Runcorn (London, The Royal Society, 1990) contains the contributions to the Discussion Meeting held at The Royal Society in February 1989. It was the first joint meeting with the Académie des Sciences in over 300 years of both their functionings.

Theoretical geophysical fluid dynamics, by A.S. Monin (Dordrecht, Boston, London, Kluwer, 1990) deals with the modern foundation of the theoretical description of natural currents in rotating stratified fluids and gases. Included is a discussion of the general circulation of planetary mantles.

The hurricane, by R.A. Pielke (London, New York, Routledge, 1990) aims to give a detailed descriptive discussion in a non-mathematical framework. Also included is an illustrated assessment of the climatology, forecasting and physical processes involved.

Satellite and radar photographs — 26 June 1990 at 1800 UTC and 27 June 1990 at 0000 UTC

The COST-73 (Co-operation in Science and Technology) pictures covering much of western Europe show radar rainfall data from several countries superimposed on infra-red cloud imagery from Meteosat. The pictures illustrate the evolution of thunderstorms on a variety of scales, some with very distinctive signatures.

At 1800 UTC (Fig. 1) a large, nearly circular, mesoscale convective system (MCS) covers much of the Massif Central in France. There are areas of heavy rainfall within the larger cloud-shield. The distinctive shape results from a merging of high-level anvil outflows from the active cells within a region of weak vertical wind-shear. The satellite image also clearly shows at least three further MCSs tied to the Alps (radar data were not available for this area). Over northern France there is a broader band of cloud and heavy (thunderstorm) rainfall associated with a convergence zone marking the northern boundary of a tongue of air with very high wet-bulb potential temperature at low levels (Fig. 2).

By 0000 UTC (Fig. 3) the MCS previously over the Massif Central has moved north-east ahead of a weak short-wave upper-level trough (Fig. 4) and merged with an intensifying system on its south-east flank. Meanwhile the band of precipitation further north has edged south and also intensified. Violent storms within this band caused serious flooding on the Paris Metro.

A.J. Waters

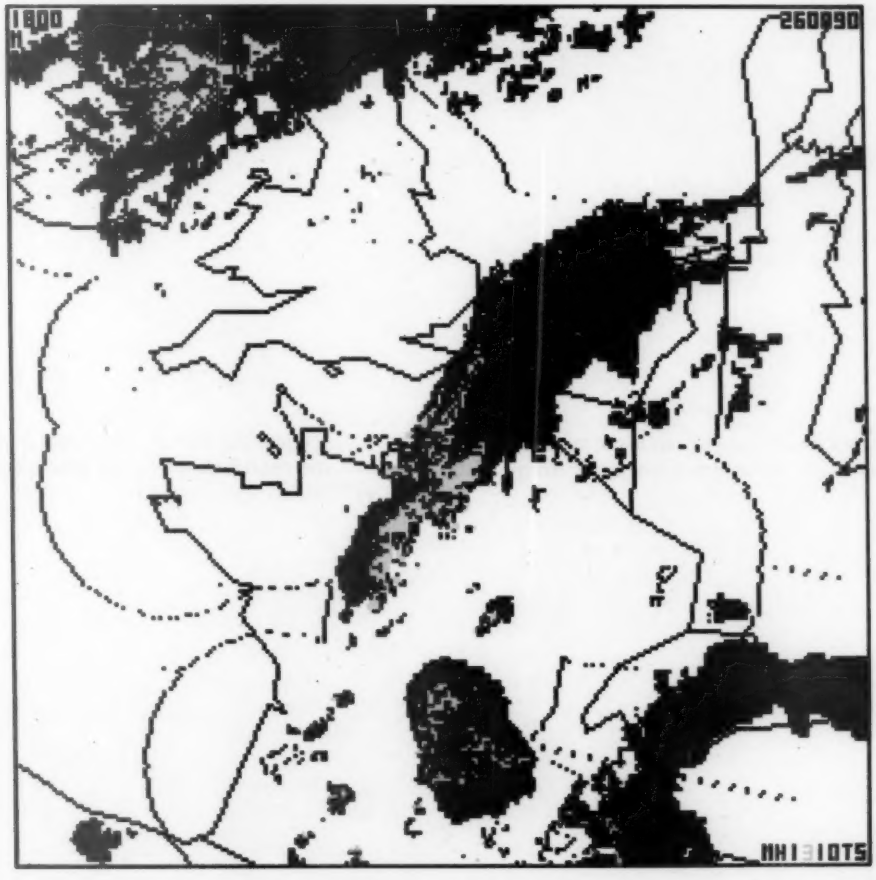

Figure 1. COST-73 satellite and radar image for 1800 UTC on 26 June 1990. Dark blue represents cloud tops with temperatures between −15 and −45 °C, and pink <−45 °C. Rainfall intensities (mm h^{-1}) are shown as follows: green < 1, yellow 1–3, red 3–10, light blue 10–30 and black > 30. Coastlines, national boundaries and the limits of radar coverage are shown in black.

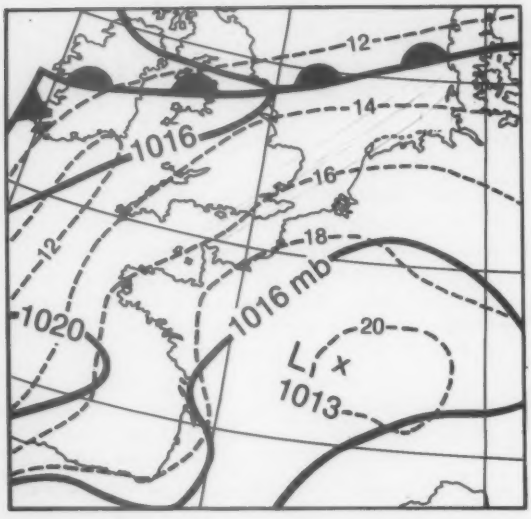

Figure 2. Surface analysis for 1800 UTC on 26 June 1990 with 850 mb wet-bulb potential temperature isotherms (°C) shown as dashed lines.

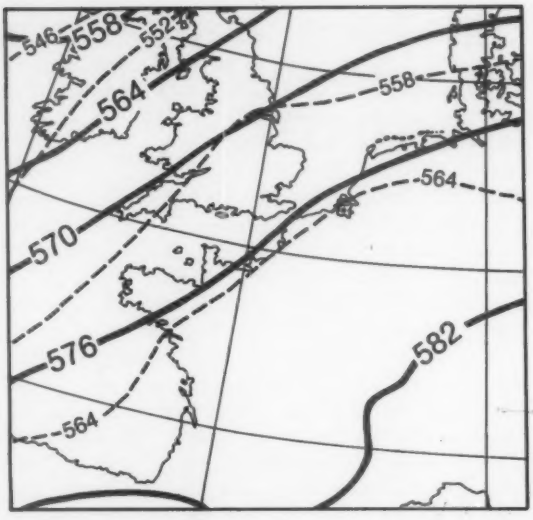

Figure 4. Upper-air analysis for 0000 UTC on 27 June 1990. Solid lines depict 500 mb contours and dashed lines the 1000–500 mb thickness (both in decametres).

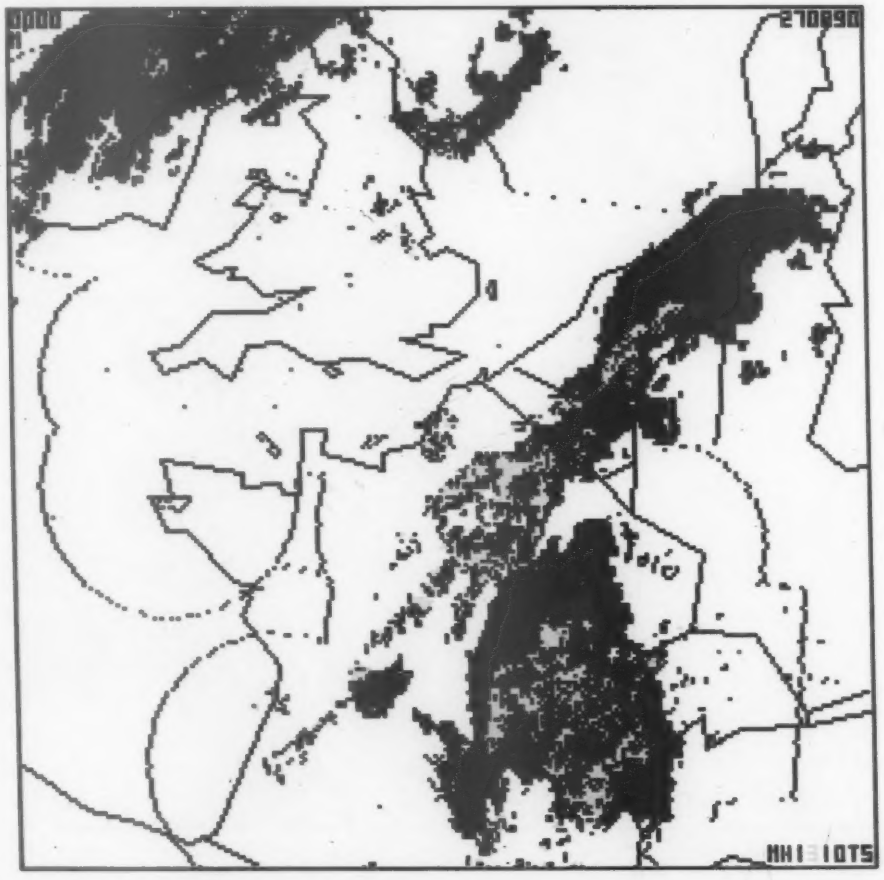

Figure 3. As Fig. 1 but for 0000 UTC on 27 June 1990.

GUIDE TO AUTHORS

Content

Articles on all aspects of meteorology are welcomed, particularly those which describe results of research in applied meteorology or the development of practical forecasting techniques.

Preparation and submission of articles

Articles, which must be in English, should be typed, double-spaced with wide margins, on one side only of A4-size paper. Tables, references and figure captions should be typed separately. Spelling should conform to the preferred spelling in the *Concise Oxford Dictionary* (latest edition). Articles prepared on floppy disk (Compucorp or IBM-compatible) can be labour-saving, but only a print-out should be submitted in the first instance.

References should be made using the Harvard system (author/date) and full details should be given at the end of the text. If a document is unpublished, details must be given of the library where it may be seen. Documents which are not available to enquirers must not be referred to, except by 'personal communication'.

Tables should be numbered consecutively using roman numerals and provided with headings.

Mathematical notation should be written with extreme care. Particular care should be taken to differentiate between Greek letters and Roman letters for which they could be mistaken. Double subscripts and superscripts should be avoided, as they are difficult to typeset and read. Notation should be kept as simple as possible. Guidance is given in BS 1991: Part 1: 1976, and *Quantities, Units and Symbols* published by the Royal Society. SI units, or units approved by the World Meteorological Organization, should be used.

Articles for publication and all other communications for the Editor should be addressed to: The Chief Executive, Meteorological Office, London Road, Bracknell, Berkshire RG12 2SZ and marked 'For Meteorological Magazine'.

Illustrations

Diagrams must be drawn clearly, preferably in ink, and should not contain any unnecessary of irrelevant details. Explanatory text should not appear on the diagram itself but in the caption. Captions should be typed on a separate sheet of paper and should, as far as possible, explain the meanings of the diagrams without the reader having to refer to the text. The sequential numbering should correspond with the sequential referrals in the text.

Sharp monochrome photographs on glossy paper are preferred; colour prints are acceptable but the use of colour is at the Editor's discretion.

Copyright

Authors should identify the holder of the copyright for their work when they first submit contributions.

Free copies

Three free copies of the magazine (one for a book review) are provided for authors of articles published in it. Separate offprints for each article are not provided.

September 1990

Editor: F.E. Underdown
Editorial board: R.J. Allam, R. Kershaw, W.H. Moores, P.R.S. Salter

Vol. 119
No. 1418

Contents

Contributions: It is requested that all communications to the Editor and books for review be addressed to the Chief Executive, Meteorological Office, London Road, Bracknell, Berkshire RG12 2SZ, and marked 'For *Meteorological Magazine*'. Contributors are asked to comply with the guidelines given in the *Guide to authors* which appears on the inside back cover. The responsibility for facts and opinions expressed in the signed articles and letters published in *Meteorological Magazine* rests with their respective authors.

Subscriptions: Annual subscription £30.00 including postage; individual copies £2.70 including postage. Applications for postal subscriptions should be made to HMSO, PO Box 276, London SW8 5DT; subscription enquiries 071–873 8499.

Back numbers: Full-size reprints of Vols 1–75 (1866–1940) are available from Johnson Reprint Co. Ltd, 24–28 Oval Road, London NW1 7DX. Complete volumes of *Meteorological Magazine* commencing with volume 54 are available on microfilm from University Microfilms International, 18 Bedford Row, London WC1R 4EJ. Information on microfiche issues is available from Kraus Microfiche, Rte 100, Milwood, NY 10546, USA.

ISBN 0 11 728669 9 ISSN 0026–1149